Electronic Supplementary Material (ESI) for Journal of Materials Chemistry C.

Supporting Information

Metal–organic frameworks-derived CdS-NiO heterostructure with modulated morphology and enhanced photocatalytic hydrogen evolution activity in pure water

Ye-Zhan Lin, Kai Wang, Yu Zhang, Yi-Chuan Dou, Yi-Jin Yang, Mei-Ling Xu, Yanju Wang, Fu-Tian Liu and Kui Li*

School of Materials Science and Engineering, University of Jinan, Jinan 250022, P. R. China Email: mse_lik@ujn.edu.cn.

Materials and General Methods.

The $Cd(NO_3)_2 \cdot 4H_2O$, $Ni(NO_3)_2 \cdot 6H_2O$, CH_4N_2S, 1,3,5-benzenetricarboxylic acid ($C_6H_3(COOH)_3$), *N*,*N*-Dimethylformamide (DMF) and polyvinyl pyrrolidone (PVP) (Shanghai Macklin Biochemical Technology Co., Ltd) are analytical grade and used as received without further purification.

The powder X-ray diffraction (PXRD) patterns were recorded on a D/max 2500 VL/PC diffractometer (Japan) equipped with graphite monochromatized Cu Kα radiation (λ = 1.54060 Å), and the corresponding work voltage and current was 40 kV and 100 mA, respectively. Fourier transform infrared spectroscopy (FTIR) was collected on a Thermo Scientific Nicolet iS10 spectrometer. The transmission electron microscopy (TEM) and high-resolution TEM (HRTEM) images were recorded on JEOL-2100F apparatus at an accelerating voltage of 200 kV. Surface morphologies of the CdS-NiO heterostructures were examined by a scanning electron microscope (SEM, JSM-7600F) at an acceleration voltage of 10 kV, and the elemental mapping was performed with JSM-5160LV-Vantage typed energy dispersive X-ray spectroscopy (EDS) spectrometer. Element content analysis was tested on an inductively coupled plasma (ICP) spectroscope (Prodigy, Leeman, America). The UV−Vis absorption and diffused reflectance spectra were recorded using a Cary 5000 UV-Vis spectrometer (Viarian, USA) with $BaSO_4$ as a reflectance standard. Nitrogen adsorption-desorption isotherms were measured at 77 K on a Quantachrome Instruments Autosorb AS-6B. The pore size distributions were measured by the Barrett-Joyner-Halenda (BJH) method. Steady photoluminescence (PL) emission spectra were tested by a luminescmce spectrophotometer (QM-400, PTI) with 350 nm excitation wavelength.

All the electrochemical experiments were conducted on the electrochemical station (Bio-Logic SP-150) in a three-electrode system at room temperature with a glassy carbon electrode (3 mm in diameter), (sheet resistance 20−25 Ω/square) as the working electrode, a platinum wire as the auxiliary electrode, and an Ag/AgCl electrode as the reference electrode. For the electrochemical measurements, 4 mg of

the catalysts were dispersed in 2 mL of 9:1 v/v water/Nafion by sonication to form a homogeneous ink. Typically, 5 μL well-dispersed catalysts were covered on the glassy carbon electrode and then dried in an ambient environment for measurements. The electrocatalyst was prepared with a catalyst loading of 0.14 mg cm^{-2}. The electrolyte of transient photocurrent responses experiments, electrochemical impedance spectroscopy (EIS), and Mott-Schottky (M-S) was 0.5 M Na_2SO_4 aqueous solution, and the electrolyte of linear sweep voltammetry (LSV) was 1M KOH solutions for the HER and OER results, respectively. EIS was performed at an impressed voltage of -0.3 eV, for voltage ranging from -2.5 V to 2.5 V. M-S was measured for a scan voltage ranging from -1 V to 0.5 V at 500-2000 Hz. The transient photocurrent responses measurement was performed under full light irradiation, and the LSV obtained at a scan rate of 1 mV/s.

Photocatalytic hydrogen evolution

The photocatalytic H_2-production experiments were performed via a photocatalytic H_2-production activity evaluation system (CEL-SPH2N, CEAULight, China) in a 150 mL Pyrex flask, and the openings of the flask were sealed with silicone rubber septum. A 300 W xenon arc lamp through a UV-cut off filter with a wavelength range of 420 ~ 800 nm, which was positioned 13 cm away from the reaction solution, was used as a visible light source to trigger the photocatalytic reaction. The focused intensity on the flask was ~ 200 $mW \cdot cm^{-2}$ measured by a FZ-A visible-light radiometer (photoelectric instrument factory of Beijing Normal University, China). In a typical photocatalytic H_2-production experiment, 20 mg of the as-prepared photocatalyst was suspended in 50 mL of 0.35 M Na_2S and 0.25 M Na_2SO_3 mixed aqueous solution. Before irradiation, the system was vacuumed for 5 min via the vacuum pump to completely remove the dissolved oxygen. A continuous magnetic stirrer (800 r/m) was applied at the bottom of the reactor to keep the photocatalyst particles in suspension during the experiments. The H_2 content was analyzed by gas chromatography (GC-7900, CEAULight, China). The photocatalytic stability was performed in the same processing parameters, and the gas was removed every 3 hours. The photocatalytic hydrogen production in pure water was performed for 9 hours under UV-vis and visible light irradiation, and the concentration of H_2O_2 was determined by a colorimetric titration method based on the formation of a yellow coloured complex Ti^{IV}–H_2O_2, using a UV/Vis spectrophotometer at 410 nm as reported in previous publication.

Supporting Figures

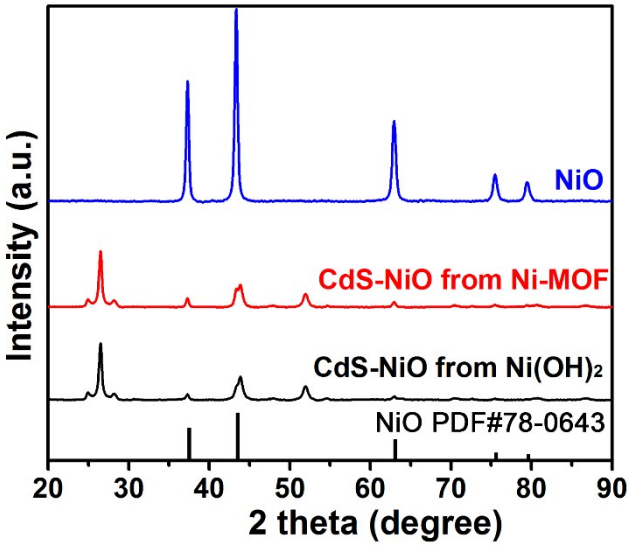

Fig. S1. The comparison results of the X-ray diffraction patterns of NiO, CdS-NiO derived from inorganic $Ni(OH)_2$ (CdS-NiO-I) and Ni-MOF (CdS-NiO-M). Both the CdS-NiO-I and CdS-NiO-M exhibited obvious CdS/NiO heterostructure, which was similar to that of CdS-NiO prepared with PVP surface modification with Ni-MOF as the precursor for NiO.

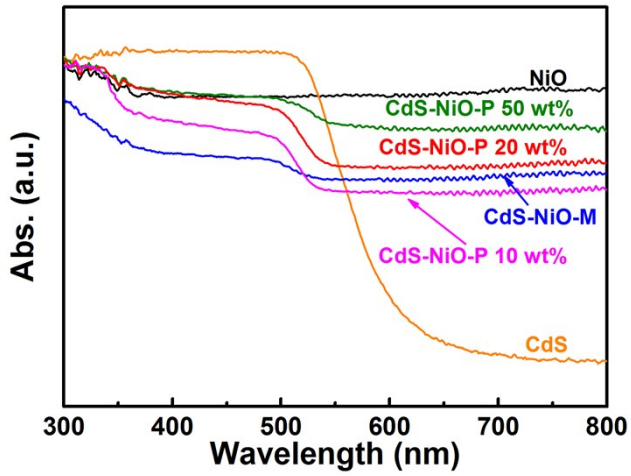

Fig. S2. The UV−visible diffuse reflection spectra of the CdS-NiO-P embedded different amount of NiO, with the CdS, NiO and CdS-NiO-M as the reference samples. The adoption of NiO dramatically improved the visible light absorption capacity.

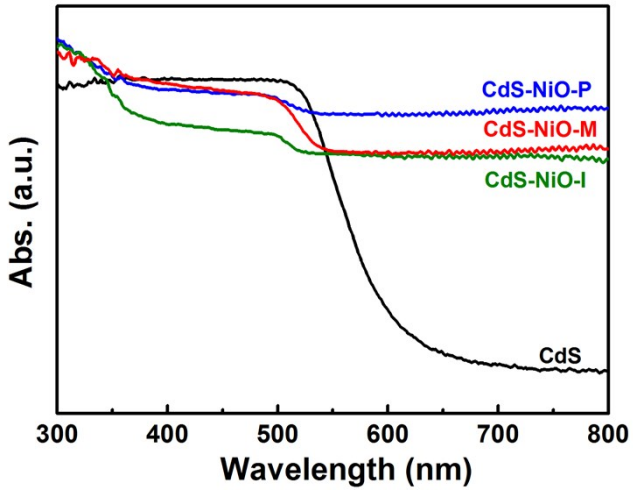

Fig. S3. The comparison results of the UV−visible diffuse reflection spectra of CdS-NiO prepared with inorganic $Ni(OH)_2$ (CdS-NiO-I), Ni-MOF (with and without PVP surface modification as CdS-NiO-P and CdS-NiO-M, respectively) as precursors. Compared with the single bandgap of CdS, all the CdS-NiO samples exhibited obvious two band edges, confirming the formation of CdS/NiO heterostructure. Moreover, the relative order of absorption capacity of visible light for these samples was found to be: CdS-NiO-P > CdS-NiO-M > CdS-NiO-I, indicating both the MOF-templated porous microstructure and the uniformly distribution of CdS-NiO could increase the absorption of visible light.

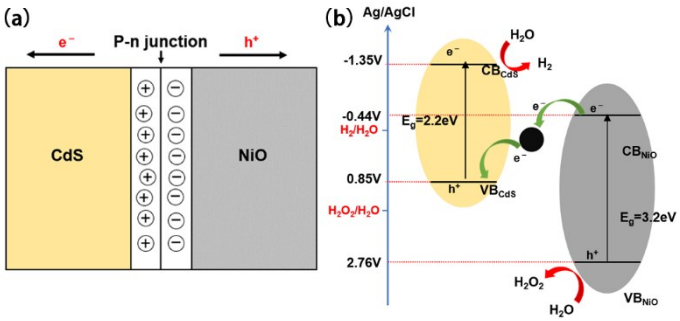

Fig. S4. (a) possible mechanism for separation of the charge carriers over CdS-NiO-P. (b) Schematic for charge transfer at p-n junction.

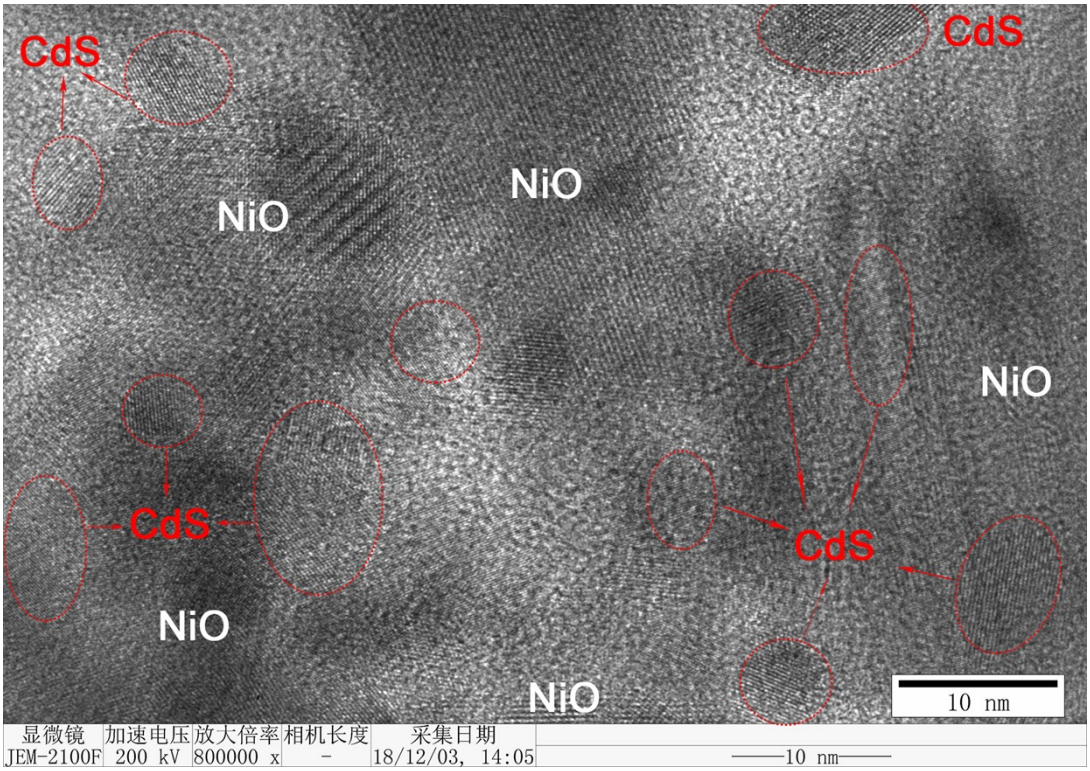

Fig. S5. The HRTEM image of the CdS-NiO-P, which further confirmed the uniformly distributed of CdS nanoparticles over the porous NiO.

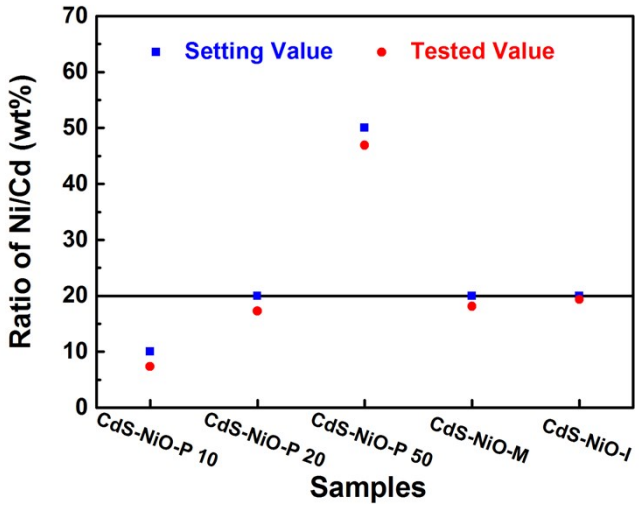

Fig. S6. The ratio of Ni/Cd of CdS-NiO-P with different content of Ni, CdS-NiO-M and CdS-NiO-I tested by inductively coupled plasma (ICP) spectroscope. The tested values were very similar to those of the setting value, and the optimal CdS-NiO-I, CdS-NiO-M and CdS-NiO-M also exhibited very close Cd/Ni ratio.

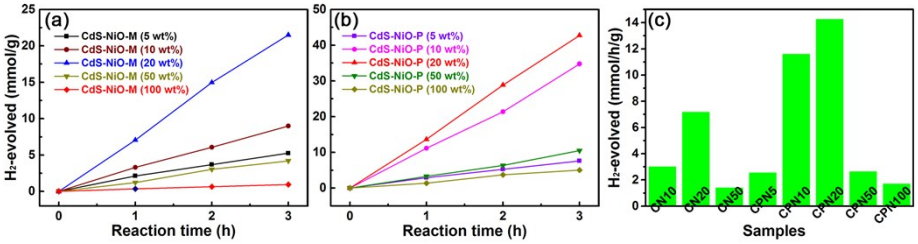

Fig. S7. The time dependence of the photocatalytic hydrogen production activity of the CdS-NiO (a) without and (b) with PVP surface modification, and the (c) comparison results of the CdS-NiO-M (CNx) and CdS-NiO-P (CPNy) with x, y as the concentration (weight ratio) of NiO.

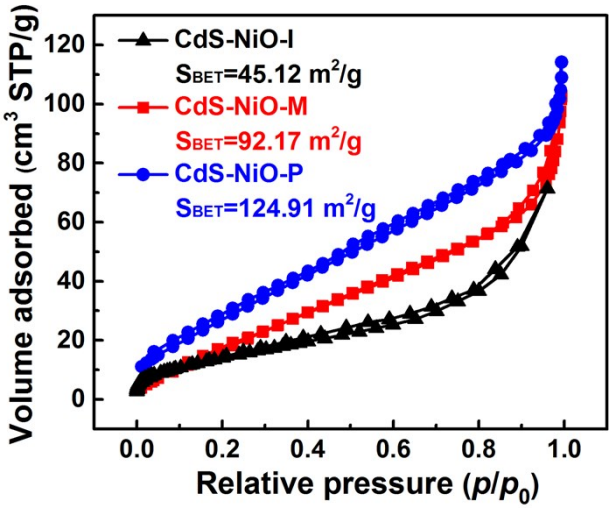

Fig. S8. The nitrogen adsorption/ desorption isotherms and the specific surface area of the CdS-NiO-I, CdS-NiO-M and CdS-NiO-P heterostructure samples. The relative order of nitrogen adsorption/ desorption isotherms and the specific surface area for these samples was found to be: CdS-NiO-P > CdS-NiO-M > CdS-NiO-I, indicating both the MOF-templated porous microstructure and the uniformly distribution of CdS-NiO could increase the specific surface area and the number of exposed active sites.

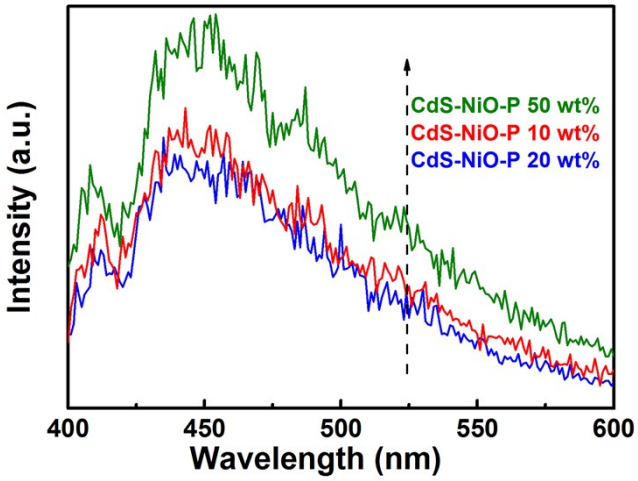

Fig. S9. The room temperature photoluminescence (PL) spectra of the CdS-NiO-P samples with different amount of NiO.

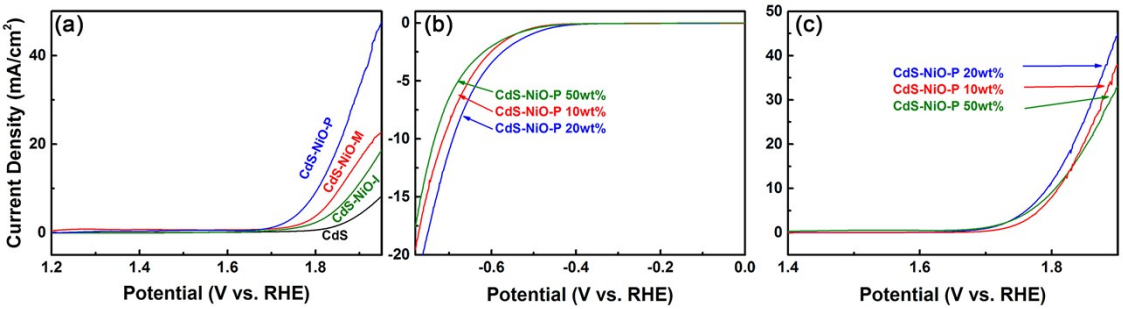

Fig. S10. (a) Electrocatalytic HER of the CdS, NiO, CdS-NiO and CdS-NiO-P samples, and electrocatalytic (b) HER and (c) OER of the CdS-NiO-P samples with different amount of NiO.

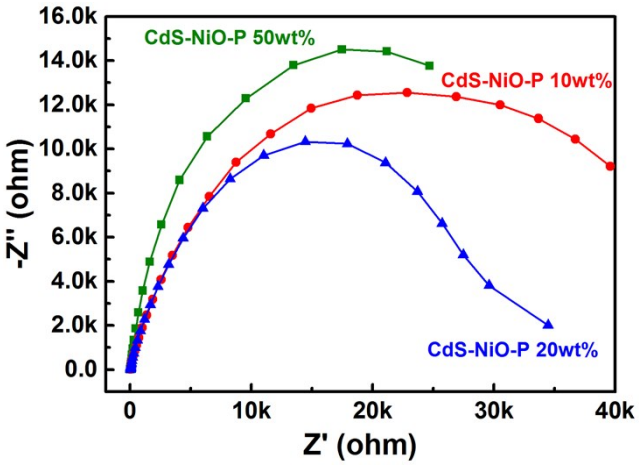

Fig. S11. The electrochemical impedance spectroscopy (EIS) of the CdS-NiO-P samples with different amount of NiO.

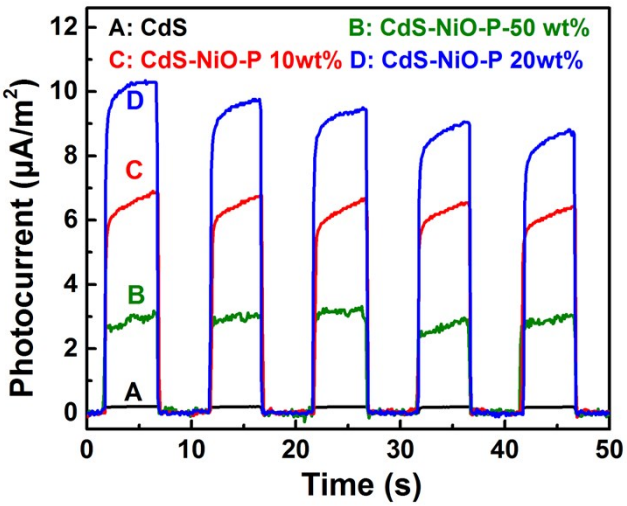

Fig. S12. The transient photocurrent response of the CdS-NiO-P samples with different amount of NiO.

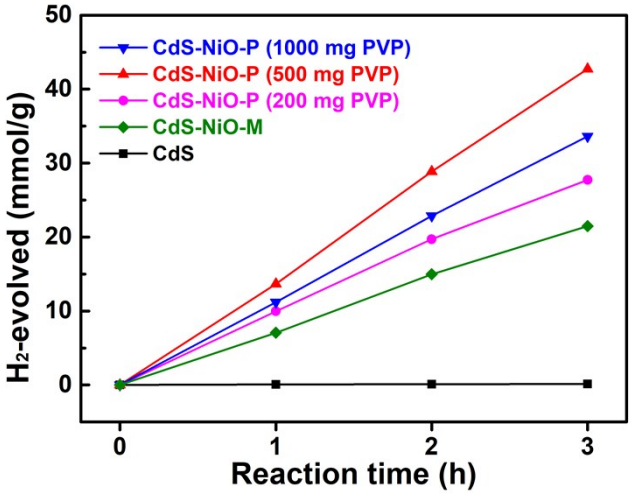

Fig. S13. The photocatalytic hydrogen evolution rate of CdS-NiO modulated by different amounts of PVP under visible light irradiation.